Optimal Waveform Selection for Tracking Systems

David J. Kershaw, *Student Member, IEEE,* and Robin J. Evans, *Member, IEEE*

Abstract—**In this paper we investigate adaptive waveform selection schemes where selection is based on overall target tracking system performance. Optimal receiver assumptions allow the inclusion of transmitted waveform specification parameters in the tracking subsystem defining equations. We give explicit expressions for two one-step ahead optimization problems for a single target in white Gaussian noise when the tracker is a conventional Kalman filter. These problems may be solved to yield the most improvement possible in tracking performance for each new transmitted pulse. In cases where target motion is restricted to one dimension, closed-form solutions to the local (one step ahead) waveform optimization problem have been obtained. The optimal waveform selection algorithms in this paper may be included with conventional Kalman filtering equations to form an enhanced Kalman tracker. Simulation examples are presented to illustrate the potential of the waveform selection schemes for the optimal utilization of the capabilities of modern digital waveform generators, including multiple waveform classes. The extension of the basic waveform optimization scheme to more complex tracking scenarios is also discussed.**

Index Terms—**Waveform selection, target tracking, system optimization, Kalman filters.**

I. Introduction

Little attention has been focused on the question of optimal waveform design over recent years, largely due to a perceived lack of flexibility in waveform generation techniques. With the advent of flexible digital waveform generators there is now scope for significant improvement in tracking system performance if waveform, and hence sensor, design is considered as an integral part of the overall tracking system design process. This paper reconsiders the signal design problem from a systems engineering viewpoint, allowing us to pose waveform optimization problems, where the cost functional is a measure of overall tracking system performance.

The conventional approach to tracking system design has been to treat the sensor and tracking sub-systems as completely separate entities [5, p. 3]. Here we refer to the sensor as containing both the actual transducer array, for an active sonar or radar system, and the receiver subsystem. Classically, the sensor's role has been to obtain estimates of target location for downstream processing. Any signal design was aimed at maximizing sensor performance, normally concentrating on modifying the matched filter response of the receiver to maximize resolution [12], [19], minimize the effects of mismatching [16], and optimal signal design for reverberation-limited environments [25]. A related problem is the question of signal synthesis given a desired matched filter response [9], [27]. The tracking subsystem then attempts to correlate the current measurements with the past measurement history. Tracking and data association algorithms have been extensively discussed elsewhere (e.g., [5]).

Early attempts at waveform optimization were predominantly attempts at measurement pattern optimization, mainly due to the inflexibility of waveform generators. In [8], Daum presents a comprehensive discussion of system considerations for multiple target tracking, including aspects of both measurement pattern optimization and waveform optimization. Radar signal design is approached in [1] and [21] from a control theoretic approach, subject to constraints on both average and peak transmitted power; however, the multiplicative control model employed limits the optimal waveform solutions to "on–off" measurement patterns, where the optimal signal alternates between peak-power and zero-power levels. In comparison, the waveform optimization approach used in this paper assumes a constant pulse repetition interval while allowing the actual waveform shape to vary under a constant transmitted energy constraint. This approach may be regarded as a nonlinear discrete time stochastic control problem with the waveform parameter vector as the control input.

The fundamental difference between conventional active tracking systems and the proposed tracking system is the inclusion of a waveform optimization block after the conventional tracker block as shown in Fig. 1. The general idea is not new: active tracking system receivers have exercised control over the transmitted waveform for many years, if only in crude and ad hoc ways. For example, many small sonar systems designed to hunt a single target start with a long pulse repetition interval (PRI) so as to allow target acquisition at long range, then changing to a shorter PRI as the target closes. Naturally, the feedback

Manuscript received April 8, 1993; revised September 2, 1993. This work was supported in part by the Aeronautical and Maritime Research Laboratory, Defence Science and Technology Organisation, Victoria, Australia, and by the Co-operative Research Centre for Sensor Signal and Information Processing.

D. J. Kershaw was with the Department of Communication and Electronic Engineering, Royal Melbourne Institute of Technology, Victoria, Australia. He is now with the Aeronautical and Maritime Research Laboratory, Department of Defence, Defence Science and Technology Organisation, PO Box 4331, Melbourne Vic. 3001, Australia.

R. J. Evans is with the Department of Electrical and Electronic Engineering, University of Melbourne, Victoria, Australia.

IEEE Log Number 9405090.

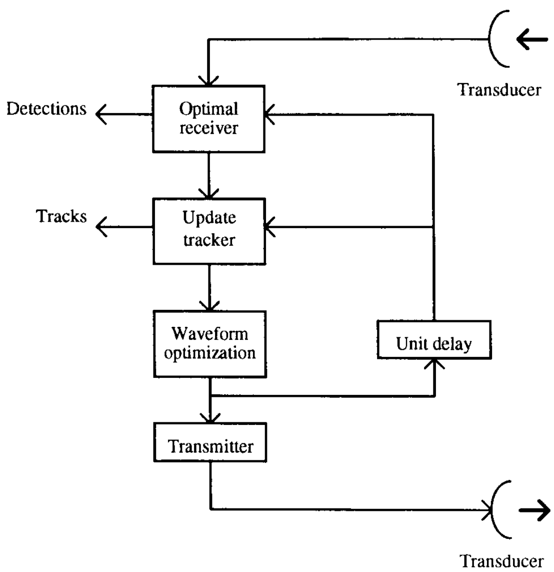

Fig. 1. Proposed active tracking system.

loop shown in Fig. 1 is not needed in this situation as the waveform sequence changes at predetermined ranges. In the proposed system the feedback loop is essential, as the receiver and tracker both need the last transmitted waveform parameter vector for correct operation.

Most previous attempts at a systems approach to tracking system design and analysis are classifiable as either passive systems, where the receiver and tracker are linked, or measurement pattern optimization systems. Passive sensor systems examined include systems where one or more of the receiver (detector) parameters, such as returned signal amplitude [15] or both signal amplitude and phase information [3], are explicitly contained in the target state vector. Alternative approaches have incorporated detection probabilities in the tracking filter algorithms to overcome the problem of missed detections by the receiver. A review of these algorithms can be found in [20]. Similarly, [6] details an algorithm where detection probabilities are included in the *a posteriori* probability density function for the tracking filter. Most of the above schemes are unidirectional in information flow. In [10], a feedback loop from the tracking filter to the receiver allows the detection threshold to vary according to tracking performance. Here the chosen tracking performance measure is expressed in terms of probability of detection and false alarm probabilities in the detector [5, Ch. 8]. This idea has been extended to a formulation for system performance including the presence of false target tracks [4]. An earlier related idea is presented in [17].

The main contribution of this paper is the reexamination of optimal waveform selection for active transmission tracking systems from a systems engineering viewpoint. The formulation differs from earlier work by assuming a flexible waveform generator, allowing greater control over the actual transmitted waveform, whereas previous studies [1], [8], [21] have concentrated on the magnitude and temporal separation of the transmitted pulses. Our approach yields a tracking system formulation where the tracking equations are explicitly dependent on the actual parameters of the transmitted waveform.

The layout of the paper is as follows. Section II outlines the assumptions and the general signal and target models employed in this paper. In Section III the sensor is characterized, leading to an expression for the estimation error covariance matrix that is dependent on the waveform parameters at the output of the sensor. Section IV relates the standard tracking filter equations to waveform dependent measures of tracking performance. Closed-form solutions, suitable for on-line use, to the local optimization algorithms for two tracking measures are discussed in Section V. Simulation results are presented in Section VI to illustrate the improvement in tracking performance using tracker-based waveform selection schemes, while in Section VII the extension of the fundamental ideas in this paper to more general tracking scenarios is discussed.

II. Problem Formulation

It is necessary to have a clear understanding of the two time frames that arise in a tracking system; one associated with the sensor, the other with the tracker. In active (as opposed to passive) tracking scenarios the sensor must perform signal processing within the time duration of a received pulse to obtain estimates of a possible target's range, radial velocity, azimuth angle, and elevation angle. Conversely, the tracker is performing information processing based on outcomes of the signal processing and must operate on an interpulse time frame.

Several assumptions are made in this formulation. Some of these have a strong physical basis, others are necessary to allow us to focus on the fundamental problem at hand. Restrictions to single target tracking and no missed detections by the sensor fall into this latter category. The problems posed by the relaxation of these latter assumptions have been extensively addressed elsewhere (e.g. [5], [7], [20]).

Constraints on transmitted waveform peak power, maximum pulse length, and constant carrier frequency all have a physical basis. For example, sonar transducers exhibit peak amplitude constraints, both because of hardware limitations and the need to avoid cavitation at the transducer to water interface. In general, the peak amplitude constraint may need to be explicitly included in the optimization problem. Under a constant energy per pulse restriction, the peak amplitude constraint results in a minimum pulse length for any given waveform class. The maximum pulse length is not waveform specific since it specifies the minimum target detection range for a single sensor system (the receiver is "blind" during waveform transmission). This is particularly important in sonar systems due to the relatively slow propagation speed of the medium. Assuming a constant carrier frequency removes one possible variable from the optimization problem, in practice this frequency would be limited by the frequency response of the transducer array. A fixed carrier frequency also simplifies any analog prefiltering employed in the radar or sonar receiver.

Constant energy per transmitted pulse and a constant data rate are typical assumptions for track-while-scan radar systems and are also valid for many active radar and sonar systems. In the context of waveform selection, the optimization problems formulated using these assumptions are possibly the simplest class of problems to solve. An immediate consequence of the constant data rate constraint is a discrete time tracking filter. The constant energy restriction allows a local optimization problem to be posed, namely, select the next transmitted waveform based on some cost at the next received pulse with no reference to previously transmitted waveforms. Neither of these restrictions can be relaxed without the introduction of a global energy budget.

We are now in a position to outline the mathematical models used for both the signal (intrapulse) processing and the information (interpulse) processing in the tracking system. Our analysis assumes a continuous time signal processor and a discrete time information processor. In modern practice the signal processor would also be a discrete time processor but we are interested in characterizing optimal receiver behavior of the signal processing, rather than specific aspects of receiver implementation.

The first model of interest is the signal model for intrapulse processing. Let a narrow-band transmitted pulse be represented by

$$s_T(t) = \sqrt{2}\ \mathrm{Re}\left\{\sqrt{E_T}\,\tilde{s}(t)e^{j\omega_c t}\right\}$$

where $\tilde{s}(t)$ is the complex envelope, ω_c is the carrier frequency (radians/sec), and E_T is the energy of the transmitted pulse. The envelope function is assumed to be normalized so that

$$\int_{-\infty}^{\infty} |\tilde{s}(t)|^2\, dt = 1.$$

The received signal due to a single target can be written as [26, p. 275]

$$s_R(t) = \sqrt{2}\ \mathrm{Re}\left\{\left[\sqrt{E_R}\,e^{j\phi}\tilde{s}(t-\tau_0)e^{j\nu_0 t} + \tilde{n}(t)\right]e^{j\omega_c t}\right\}$$

where ϕ is a random phase shift, E_R is the energy of the reflected pulse and is related to the energy of the transmitted pulse by medium attenuation and target cross section, while $\tilde{n}(t)$ is zero-mean complex white Gaussian noise with real spectral density $N_0/2$. The parameters τ_0 and ν_0 are target time delay and Doppler shift, respectively. If the one-dimensional equation of motion for the target at the moment of pulse reflection is written as $r(t) = r_0 + \dot{r}_0 t$ then τ_0, ν_0 are given by $\tau_0 = 2r_0/c$, $\nu_0 = (2\dot{r}_0/c)\omega_c$, where c is the speed of waveform propagation. These expressions for the target parameters assume that time compression due to Doppler shift can be ignored, i.e., the maximum Doppler shift is small compared to the transmission frequency ω_c [26, p. 241]. This narrowband assumption holds for most radar systems, however it is often untrue for sonar systems.

The interpulse target model is a discrete-time dynamical motion model of the form

$$\boldsymbol{x}_{k+1} = \boldsymbol{F}\boldsymbol{x}_k + \boldsymbol{G}\boldsymbol{w}_k \tag{2.1}$$

where $\boldsymbol{x}_k$ is the target state vector at time k while the measurement vector of target state at time k is given by the linear relation

$$\boldsymbol{y}_k = \boldsymbol{H}\boldsymbol{x}_k + \boldsymbol{n}_k. \tag{2.2}$$

A polar coordinate system is used for both the target dynamic motion model and the measurement model [5]. Explicit representation of the $\boldsymbol{F}$, $\boldsymbol{G}$, and $\boldsymbol{H}$ matrices for a one-dimensional tracking problem are given in Section VI. The noise vectors $\boldsymbol{w}_k$ and $\boldsymbol{n}_k$ are independent identically distributed (iid) zero-mean white Gaussian sequences with covariance matrices $\boldsymbol{Q}_k$ and $\boldsymbol{N}(\boldsymbol{\theta}_k)$ respectively; $\boldsymbol{w}_k$ allows for perturbations in the target trajectory not easily described by the dynamic model while $\boldsymbol{n}_k$ represents measurement noise. The vector $\boldsymbol{\theta}_k$ characterizes the waveform parameters for the waveform received at time k and is included in the measurement noise covariance matrix description $\boldsymbol{N}(\boldsymbol{\theta}_k)$ to show the explicit dependence of this covariance matrix on the transmitted waveform parameters.

The general waveform selection question may now be posed. Given the above signal and target models, what is the tracking filter structure and waveform parameter sequence which yields a minimum variance estimate of the target state vector $\boldsymbol{x}_k$? That is

$$\min_{\Gamma,\{\boldsymbol{\theta}_1,\cdots,\boldsymbol{\theta}_k\}\in\boldsymbol{\Theta}} E\left\{\|\boldsymbol{x}_k - \hat{\boldsymbol{x}}_k\|^2 | \boldsymbol{Z}^m\right\}$$

where $\boldsymbol{\Gamma}$ denotes the filter structure, $\boldsymbol{\Theta}$ is the set of allowed values for $\boldsymbol{\theta}$, and $\boldsymbol{Z}^m$ is the set of measurements $\{\boldsymbol{y}_1,\cdots,\boldsymbol{y}_m\}$ up to and including time $m \le k$.

III. Sensor Characterization

The sensor is characterized by knowledge of the measurement noise covariance matrix $\boldsymbol{N}(\boldsymbol{\theta})$. It is well known that the matched filter receiver generates the likelihood function, which can be used for both optimal signal detection and optimal parameter estimation [13]. Provided the received energy-to-noise ratio is sufficiently large so that estimation errors are small, then the peak of the likelihood function is an unbiased maximum likelihood estimator and the estimation errors achieve the Cramer–Rao lower bound [26, p. 300]. In this section we show that the Cramer–Rao lower bound, and hence the measurement noise covariance matrix $\boldsymbol{N}(\boldsymbol{\theta})$, can be evaluated from a knowledge of the ambiguity function for any given waveform class.

In the previous section the transmitted waveform envelope was written as $\sqrt{E_T}\,\tilde{s}(t)$, where $\tilde{s}(t)$ has unit energy. Using the same framework the received waveform envelope is

$$\tilde{r}(t) = \sqrt{E_R}\,e^{j\phi}\tilde{s}(t-\tau_0)e^{j\nu_0 t} + \tilde{n}(t), \tag{3.1}$$

where E_R is assumed to be nonrandom for the purposes of this paper. The *mean time* $\bar{t}$ and *mean frequency* $\bar{\omega}$, are given by

$$\bar{t} \triangleq \int_{-\infty}^{\infty} t|\tilde{s}(t)|^2\,dt,$$

$$\bar{\omega} \triangleq \int_{-\infty}^{\infty} \omega|\tilde{S}(\omega)|^2\,d\omega/2\pi,$$

and can be assumed to be zero (without loss of generality) for the transmitted waveform envelope [26, p. 571]. Here, $\tilde{S}(\omega)$ is the two-sided Fourier transform of $\tilde{s}(t)$. A zero-mean frequency is equivalent to the transmitted waveform envelope having a zero carrier frequency (as should be the case for analytic signal representation), while a zero mean time condition will be met by any symmetric waveform centered at the time origin. In the absence of noise the received waveform will have $\bar{t} = \tau_0$ and $\bar{\omega} = \nu_0$, where τ_0 and ν_0 denote the true target time delay and Doppler shift, respectively.

The ambiguity function $A(\tau - \tau_0, \nu - \nu_0)$ corresponding to the received waveform is defined as [27]

$$A(\tau - \tau_0, \nu - \nu_0) \triangleq \int_{-\infty}^{\infty} \tilde{s}(t - (\tau - \tau_0)/2) \cdot \tilde{s}^*(t + (\tau - \tau_0)/2)e^{-j(\nu-\nu_0)t}\,dt,$$

and has a maximum at the true target position (τ_0, ν_0). It is often convenient to choose the time and frequency origins so that $\bar{t} = \bar{\omega} = 0$. Thus letting $\tau' = \tau - \tau_0$ and $\nu' = \nu - \nu_0$ the ambiguity function becomes

$$A(\tau', \nu') = \int_{-\infty}^{\infty} \tilde{s}(t - \tau'/2)\tilde{s}^*(t + \tau'/2)e^{-j\nu' t}\,dt, \quad (3.2)$$

with the equivalent frequency domain form

$$A(\tau', \nu') = \int_{-\infty}^{\infty} S(\omega - \nu'/2)S^*(\omega + \nu'/2)e^{-j\omega\tau'}\,d\omega/2\pi. \quad (3.3)$$

The first step in determining the Cramer–Rao lower bound for the estimation error variance of an unbiased estimator is calculation of the Fisher information matrix. If we restrict our attention to tracking scenarios with measurement vector $y = [r\ \dot{r}]^T$ the only parameters to be estimated by the receiver are time delay τ and Doppler shift ν. In this case the Fisher information matrix is given by

$$J = \frac{2E_R}{N_0}\begin{bmatrix} \overline{\omega^2} - (\bar{\omega})^2 & \overline{\omega t} - \bar{\omega}\,\bar{t} \\ \overline{\omega t} - \bar{\omega}\,\bar{t} & \overline{t^2} - (\bar{t})^2 \end{bmatrix}, \quad (3.4)$$

where the elements of the information matrix are related to the second derivatives of the ambiguity function evaluated at the true target position [26, pp. 297–300] as follows:

$$\overline{\omega^2} - (\bar{\omega})^2 = -\left.\frac{\partial^2 A(\tau, \nu)}{\partial \tau^2}\right|_{\substack{\tau=\tau_0,\\ \nu=\nu_0}} \quad (3.5)$$

$$\overline{\omega t} - \bar{\omega}\,\bar{t} = -\left.\frac{\partial^2 A(\tau, \nu)}{\partial \tau\,\partial \nu}\right|_{\substack{\tau=\tau_0,\\ \nu=\nu_0}} \quad (3.6)$$

$$\overline{t^2} - (\bar{t})^2 = -\left.\frac{\partial^2 A(\tau, \nu)}{\partial \nu^2}\right|_{\substack{\tau=\tau_0.\\ \nu=\nu_0}} \quad (3.7)$$

The inverse of the Fisher information matrix is the Cramer–Rao lower bound on the error covariance matrix for unbiased estimates [26, p. 300]. Since the maximum likelihood estimates are asymptotically jointly Gaussian with covariance matrix J^{-1} [26, p. 301], and as we are restricting our attention to cases where the signal-to-noise ratio is sufficient to neglect any ambiguity function sidelobes, then J^{-1} is a suitable characterization of the optimal receiver for optimal waveform selection. It is now only necessary to define the relationship between the receiver estimation parameter vector and the tracking system measurement vector y to complete the specification of the measurement noise covariance matrix $N(\boldsymbol{\theta})$.

Lemma 3.1: The measurement noise covariance matrix is given by $E[(y - \bar{y})(y - \bar{y})^T] = N(\boldsymbol{\theta}) = TJ^{-1}T^T$, where J Is the Fisher information matrix ($E[(\boldsymbol{\alpha} - \bar{\boldsymbol{\alpha}})(\boldsymbol{\alpha} - \bar{\boldsymbol{\alpha}})^T] = J^{-1}$) and T is a transformation matrix between the receiver estimation parameter vector $\boldsymbol{\alpha}$ and the tracking system measurement vector, $y = T\boldsymbol{\alpha}$.

The contribution of the signal-to-noise ratio η can be separated from the contribution of the waveform parameter vector in the Fisher information matrix. Expressing the Fisher information matrix as $J = \eta U(\boldsymbol{\theta})$, where $\eta = 2E_R/N_0$ is the signal-to-noise ratio, then the elements of the symmetric matrix $U(\boldsymbol{\theta})$ are

$$u_{11} = \overline{\omega^2} - (\bar{\omega})^2 = \int_{-\infty}^{\infty} \omega^2|\tilde{S}(\omega)|^2\,d\omega/2\pi, \quad (3.8)$$

$$u_{12} = u_{21} = \overline{\omega t} - \bar{\omega}\bar{t} = \int_{-\infty}^{\infty} t\varphi'(t)|\tilde{s}(t)|^2\,dt, \quad (3.9)$$

$$u_{22} = \overline{t^2} - (\bar{t})^2 = \int_{-\infty}^{\infty} t^2|\tilde{s}(t)|^2\,dt. \quad (3.10)$$

The waveform envelope has been written as $\tilde{s}(t) = |\tilde{s}(t)|\exp(j\varphi(t))$ in obtaining the final expression for u_{12} (see Appendix A). All elements of $U(\boldsymbol{\theta})$ are real valued constants for any given waveform. Hence, using Lemma 3.1, for cases where the tracking system measurement vector is $y = [r\ \dot{r}]^T$, (receiver parameter vector is $\boldsymbol{\alpha} = [\tau\ \nu]^T$), the measurement noise covariance matrix can be shown to be

$$N(\boldsymbol{\theta}) = \frac{1}{\eta}TU^{-1}T, \quad (3.11)$$

where $T = \mathrm{diag}(c/2, c/2\omega_c)$. This expression for $N(\boldsymbol{\theta})$ is only valid under the assumption of constant energy per transmitted waveform, otherwise the tracking system would also have control of the signal-to-noise ratio with η then one element of the waveform parameter vector $\boldsymbol{\theta}$.

The following properties are relevant only to the measurement noise covariance matrix in (3.11) for constant transmitted energy per waveform and $y = [r \ \dot{r}]^T$.

Lemma 3.2: The determinant of the measurement noise covariance matrix has an upper bound given by

$$\det N(\boldsymbol{\theta}) \leq \frac{c^4}{4\omega_c^2\eta^2}.$$

Proof: From [13, p. 20], assuming $\bar{t} = \bar{\omega} = 0$, we have

$$\det U = \overline{\omega^2}\,\overline{t^2} - \left(\overline{\omega t}\right)^2 \geq 1/4. \tag{3.12}$$

By writing the determinant of the measurement noise covariance matrix as

$$\begin{aligned}\det N(\boldsymbol{\theta}) &= \eta^{-2}(\det T)^2(\det U^{-1})\\ &= \eta^{-2}(\det T)^2(\det U)^{-1},\end{aligned}$$

using (3.12), and noting that $T = \mathrm{diag}(c/2, c/2\omega_c)$ obtains the desired result. □

Two comments can be made about Lemma 3.2. Firstly, if we define the *mean square bandwidth* and *mean square duration* as

$$(\Delta\omega)^2 \triangleq \overline{\omega^2} - (\bar{\omega})^2$$

and

$$(\Delta t)^2 \triangleq \overline{t^2} - (\bar{t})^2$$

respectively, then (3.12) implies $\Delta\omega \cdot \Delta t \geq 1/2$, which is the well-known "uncertainty relation," [13, p. 20], and implies that we cannot simultaneously produce a pulse that is narrow in both duration Δt and bandwidth $\Delta\omega$.

The second observation is that the upper bound on $\det N(\boldsymbol{\theta})$ is independent of the waveform parameter vector $\boldsymbol{\theta}$. As demonstrated in Appendix B, $\det N(\boldsymbol{\theta})$ is also independent of $\boldsymbol{\theta}$ for individual waveform classes with the upper bound on $\det N(\boldsymbol{\theta})$ reached for Gaussian amplitude-modulated waveforms.

Definition: A waveform is said to belong to waveform class C if

1) $\boldsymbol{\theta} \in \boldsymbol{\Theta}_C$,
2) $\det N(\boldsymbol{\theta}) = \gamma_c/\eta^2$,

where $\boldsymbol{\Theta}_C$ is the set of permissible waveform parameter vectors for the class, γ_c is a class specific constant, and $N(\boldsymbol{\theta})$ is the measurement noise covariance matrix for the waveform class.

Lemma 3.3 presents one furthe rproperty of measurement noise covariance matrices within a waveform class C for a single transmitted waveform (η is constant).

Lemma 3.3: $\forall \boldsymbol{\theta}_1, \boldsymbol{\theta}_2 \in \boldsymbol{\Theta}_C \sim \exists \boldsymbol{\theta}_1$: $N(\boldsymbol{\theta}_1) < N(\boldsymbol{\theta}_2)$.

Proof: See Appendix C.

IV. Tracker Characterization

The aim of the tracking filter is to obtain an estimate of the target state x_k from a set of noisy measurements such that the mean square error signal is minimized. Two options are available for the design of the tracking filter; with or without additional constraints [2]. The optimal solution is to seek a filter structure that solves the optimization problem posed in Section II, necessitating a search over both the possible filter structures and the waveform parameter space $\boldsymbol{\Theta}$. In general this is a difficult problem since the measurement noise covariance matrix is a waveform specific nonlinear function of the waveform parameter vector $\boldsymbol{\theta}$. A more tractable design philosophy is to constrain the filter to be linear.

Consider the linear target and measurement model presented in Section II. Due to the dependence of the measurement noise covariance matrix on $\boldsymbol{\theta}_k$, the Kalman filter equations are also explicitly dependent on $\boldsymbol{\theta}_k$. Specifically,

$$\begin{aligned}S_k(\boldsymbol{\theta}_k) &= HP_{k/k-1}H^T + N(\boldsymbol{\theta}_k),\\ K_k(\boldsymbol{\theta}_k) &= P_{k/k-1}H^TS_k^{-1}(\boldsymbol{\theta}_k),\\ \hat{x}_{k/k}(\boldsymbol{\theta}_k) &= \hat{x}_{k/k-1} + K_k(\boldsymbol{\theta}_k)\left(y_k - H\hat{x}_{k/k-1}\right),\\ P_{k/k}(\boldsymbol{\theta}_k) &= P_{k/k-1} - K_k(\boldsymbol{\theta}_k)S_k(\boldsymbol{\theta}_k)K_k^T(\boldsymbol{\theta}_k),\\ \hat{x}_{k+1/k}(\boldsymbol{\theta}_k) &= F\hat{x}_{k/k}(\boldsymbol{\theta}_k),\\ P_{k+1/k}(\boldsymbol{\theta}_k) &= FP_{k/k}(\boldsymbol{\theta}_k)F^T + GQ_kG^T.\end{aligned}$$

Unless otherwise noted this dependence on $\boldsymbol{\theta}_k$ is assumed throughout the remainder of the paper.

The covariance update equations in the Kalman filter are dependent on both Q_k (assumed known for all k) and $N(\boldsymbol{\theta}_k)$. In Section III we derived a lower bound on the measurement noise covariance matrix that is dependent only on the background noise level and on the transmitted waveform parameter vector. Hence, the measurement noise covariance matrix at time $k+1$ is known once the next waveform parameter vector is selected, thus allowing a prediction to be made of the smoothed tracking error covariance matrix at time $k+1$. This matrix is given by

$$\begin{aligned}P_{k+1/k+1}(\boldsymbol{\theta}_{k+1}) &= P_{k+1/k} - P_{k+1/k}H^T\\ &\quad\times\left(HP_{k+1/k}H^T + N(\boldsymbol{\theta}_{k+1})\right)^{-1}HP_{k+1/k},\end{aligned} \tag{4.1}$$

where the expressions for $S_{k+1}(\boldsymbol{\theta}_{k+1})$ and $K_{k+1}(\boldsymbol{\theta}_{k+1})$ have been included in full to show the dependence of the tracking error covariance on the measurement noise covariance matrix. The only unknown in (4.1) is the waveform parameter vector $\boldsymbol{\theta}_{k+1}$, thus providing us with a means of selecting the next transmitted waveform.

Having expressed the future smoothed tracking error covariance matrix in terms of the transmitted waveform parameters the next problem is the choice of appropriate optimization criteria. Since the tracking error is represented by a covariance matrix it would be desirable to minimize the "whole" matrix [21]. The situation has a clear geometric interpretation if the concept of an error ellipsoid is used; an $n \times n$ positive definite covariance matrix defines an n-dimensional ellipsoid that is a contour of constant probability of error [26, p. 298]. In this context a covariance $P(\boldsymbol{\theta}_1)$, obtained from the waveform defined by $\boldsymbol{\theta}_1$, is superior to a covariance $\boldsymbol{P}(\boldsymbol{\theta}_2)$, obtained from the waveform defined by $\boldsymbol{\theta}_2$, if $\boldsymbol{P}(\boldsymbol{\theta}_2) - \boldsymbol{P}(\boldsymbol{\theta}_1)$ is positive definite (assuming $\boldsymbol{\theta}_1, \boldsymbol{\theta}_2 \in \boldsymbol{\Theta}_C$). However, $\boldsymbol{P}(\boldsymbol{\theta}_2) - \boldsymbol{P}(\boldsymbol{\theta}_1)$ cannot be nonnegative definite in general as shown below and alternative optimization criteria must be considered.

Lemma 4.1: $\forall \boldsymbol{\theta}_1, \boldsymbol{\theta}_2 \in \boldsymbol{\Theta}_C \sim \exists \boldsymbol{\theta}_1\colon \boldsymbol{P}(\boldsymbol{\theta}_1) < \boldsymbol{P}(\boldsymbol{\theta}_2)$.

Proof: See Appendix D.

There is no best choice for a scalar function of the tracking error covariance matrix to use as an optimization criterion [1], [21]. Several possible criteria are discussed in [21] for a continuous time waveform optimization problem when the modulation is multiplicative. In this paper the two criteria selected have the dual attractions of a strong physical basis and of acting on more than one element of the covariance matrix at a time.

The first performance measure chosen selects the next transmitted waveform as that waveform that minimizes the mean square tracking error. For the one step ahead problem, using a Kalman tracker, this can be written as [2]

$$\boldsymbol{\theta}^*_{k+1} = \arg \min_{\boldsymbol{\theta}_{k+1} \in \boldsymbol{\Theta}} \operatorname{Tr}\left\{\boldsymbol{P}_{k+1/k+1}(\boldsymbol{\theta}_{k+1})\right\}. \tag{4.2}$$

A second tracking measure is to select the next transmitted waveform so that the volume of the tracking system validation gate is minimized.[1] Unlike the first measure, which is based in a space defined by the state vector $\boldsymbol{x}_k$, this measure is based in measurement space (defined by $\boldsymbol{y}_k$). Minimizing the validation gate volume would reduce the number of false alarms in densely cluttered or high-noise target-tracking scenarios (however we are assuming only single measurement in the validation gate for the purposes of this paper). The volume of the validation gate is directly proportional to the square root of the determinant of the measurement space covariance matrix $\boldsymbol{S}_{k+1}(\boldsymbol{\theta}_{k+1})$ [5, p. 169]. Mathematically this allows the waveform optimization problem using this measure to be written as

$$\boldsymbol{\theta}^*_{k+1} = \arg \min_{\boldsymbol{\theta}_{k+1} \in \boldsymbol{\Theta}} \det\left(\boldsymbol{S}_{k+1}(\boldsymbol{\theta}_{k+1})\right). \tag{4.3}$$

In the above derivations no allowance for scaling or weighting of individual elements of the error vector $(\boldsymbol{x}_{k+1} - \hat{\boldsymbol{x}}_{k+1})$ has been made. In [1] the cost functional $J = \operatorname{Tr}\{\boldsymbol{M}_{k+1}\boldsymbol{P}_{k+1/k+1}(\boldsymbol{\theta}_{k+1})\}$ is used to facilitate individual component penalization via the matrix $\boldsymbol{M}_{k+1}$.

V. Closed-Form Solutions

Under some circumstances it is poosible to obtain analytic solutions to the one step ahead waveform optimization problems posed in the previous section. Consider a one-dimensional tracking scenario, characterized by linear target and measurement models, with target state vector $\boldsymbol{x} = [r\ \dot{r}\ \ddot{r}]^T$ and measurement vector $\boldsymbol{y} = [r\ \dot{r}]^T$. The measurement noise covariance matrix is obtained from the classical time-frequency ambiguity function as shown in (3.11), with

$$\boldsymbol{H} = \begin{bmatrix} 1 & 0 & 0 \\ 0 & 1 & 0 \end{bmatrix}. \tag{5.1}$$

A. Minimization of Validation Gate Volume

The optimization problem for this cost functional is given by (4.3) where

$$\boldsymbol{S}_{k+1}(\boldsymbol{\theta}_{k+1}) = \boldsymbol{H}\boldsymbol{P}_{k+1/k}\boldsymbol{H}^T + \boldsymbol{N}(\boldsymbol{\theta}_{k+1}).$$

Representing the elements of $\boldsymbol{P}_{k+1/k}$ by p_{ij} and the elements of $\boldsymbol{N}(\boldsymbol{\theta}_{k+1})$ by n_{ij} (where the dependence of the n_{ij} on $\boldsymbol{\theta}_{k+1}$ is assumed), and with $\boldsymbol{H}$ as given in (5.1), we can write the determinant of $\boldsymbol{S}_{k+1}(\boldsymbol{\theta}_{k+1})$ as

$$\det(\boldsymbol{S}_{k+1}(\boldsymbol{\theta}_{k+1})) = (p_{11} + n_{11})(p_{22} + n_{22}) - (p_{12} + n_{12})^2 \tag{5.2}$$

or

$$\det(\boldsymbol{S}_{k+1}(\boldsymbol{\theta}_{k+1})) = \det\left(\boldsymbol{H}\boldsymbol{P}_{k+1/k}\boldsymbol{H}^T\right) + \det(\boldsymbol{N}(\boldsymbol{\theta}_{k+1})) + p_{11}n_{22} + p_{22}n_{11} - 2p_{12}n_{12}.$$

Denoting the elements of $\boldsymbol{\theta}_{k+1}$ by θ_i, and setting the derivatives of $\det(\boldsymbol{S}_{k+1}(\boldsymbol{\theta}_{k+1}))$ with respect to the θ_i equal to zero yields a set of simultaneous equations for possible solutions at each time step k. The equations are

$$\frac{\partial \det(\boldsymbol{S}_{k+1}(\boldsymbol{\theta}_{k+1}))}{\partial \theta_i} = \frac{\partial \det(\boldsymbol{N}(\boldsymbol{\theta}_{k+1}))}{\partial \theta_i} + p_{11}\frac{\partial n_{22}}{\partial \theta_i} + p_{22}\frac{\partial n_{11}}{\partial \theta_i} - 2p_{12}\frac{\partial n_{12}}{\partial \theta_i} = 0. \tag{5.3}$$

In many situations (for example, when $\boldsymbol{N}(\boldsymbol{\theta})$ is described by the time-frequency ambiguity function) $\det(\boldsymbol{N}(\boldsymbol{\theta}_{k+1}))$ will be independent of the θ_i, further simplifying (5.3). The optimal solution to (5.3) can be determined from the set of possible solutions by evaluating the second derivative of $\det(\boldsymbol{S}_{k+1}(\boldsymbol{\theta}_{k+1}))$, with respect to the θ_i, at each potential solution to find those solutions that minimize the cost functional. Equation (5.2) can be used to determine the best solution in the case of multiple minima.

1) Amplitude-Only Modulation: Within the class of amplitude-only modulated waveforms, the waveform for any subclass (e.g., triangular, Gaussian) can be characterized solely by a pulse length parameter λ. As shown by the two examples in Appendix B, the determinant of the measurement noise covariance matrix is independent of λ for amplitude only modulated waveforms. Using this fact, and noting that n_{12} is zero for this class of waveform, (5.3) simplifies to

$$\frac{\partial \det(\boldsymbol{S}_{k+1}(\lambda_{k+1}))}{\partial \lambda_{k+1}} = p_{11}\frac{\partial n_{22}}{\partial \lambda_{k+1}} + p_{22}\frac{\partial n_{11}}{\partial \lambda_{k+1}} = 0 \tag{5.4}$$

[1]The validation gate is a region of space around the predicted measurement $\boldsymbol{H}\hat{\boldsymbol{x}}_{k+1/k}$, such that the measurement, provided the target is detected, will be found in the gate with probability P_G. If $\boldsymbol{\nu}_{k+1} = y_{k+1} - \boldsymbol{H}\hat{\boldsymbol{x}}_{k+1/k}$ is the innovation at time $k+1$, then the validation gate is defined by $\{y_{k+1}\colon \boldsymbol{\nu}^T_{k+1}\boldsymbol{S}^{-1}_{k+1}(\boldsymbol{\theta}_{k+1})\boldsymbol{\nu}_{k+1} \le g^2\}$, where g is the "number of sigmas" for the gate [5, p. 151]. In practice, P_G is often assumed to be unity since $P_G > 0.99$ whenever $g > M^{1/2} + 2$, where M is the dimension of the measurement vector y_{k+1} [10].

where the waveform parameter vector $\boldsymbol{\theta}_{k+1}$ has been replaced with λ_{k+1}.

For a symmetric, triangular-shaped pulse, the measurement noise covariance matrix elements are (Appendix B)

$$n_{11}(\lambda_{k+1}) = c^2\lambda_{k+1}^2/(12\eta),$$
$$n_{22}(\lambda_{k+1}) = 5c^2/(2\omega_c^2\lambda_{k+1}^2\eta).$$

Using these (5.2) becomes

$$\det(\boldsymbol{S}_{k+1}(\lambda_{k+1})) = p_{11}p_{22} - p_{12}^2 + \frac{5c^4}{24\omega_c^2\eta^2} + \frac{p_{22}c^2}{12\eta}\lambda_{k+1}^2 + \frac{5p_{11}c^2}{2\omega_c^2\eta}\lambda_{k+1}^{-2}, \quad (5.5)$$

which is quadratic in λ_{k+1}^2. Hence, in this case there is a single optimal solution to (5.3) since the second derivative of (5.5) with respect to λ_{k+1} is positive for all λ_{k+1}. Substituting for n_{11} and n_{22} in (5.3) yields the optimal pulse length for the triangular pulse,

$$\lambda_{k+1}^*(\text{Triangular}) = \left(\frac{30p_{11}}{\omega_c^2 p_{22}}\right)^{1/4}.$$

The positive root has been used since the pulse length must be real.

Similar calculations may be performed for a pulse with Gaussian amplitude modulation to obtain

$$\lambda_{k+1}^*(\text{Gaussian}) = \left(\frac{p_{11}}{\omega_c^2 p_{22}}\right)^{1/4}.$$

It is interesting to note that the optimal solutions are independent of both signal-to-noise ratio and waveform propagation speed.

2) Amplitude and Linear Frequency Modulation: This class of waveform is characterized by both a pulse length parameter λ, and a linear frequency sweep rate parameter b, where b has dimensions rad/sec^2. The waveform parameter vector, for the waveform transmitted at time k (received at time $k + 1$), is now $\boldsymbol{\theta}_{k+1} = [\lambda_{k+1} \; b_{k1}]^T$.

Consider a linear frequency modulated (LFM) waveform pulse with Gaussian amplitude modulation. The elements of the measurement noise covariance matrix can be shown to be (Appendix B)

$$n_{11}(\lambda_{k+1}) = c^2\lambda_{k+1}^2/(2\eta),$$
$$n_{12}(\lambda_{k+1}, b_{k+1}) = -c^2 b_{k+1}\lambda_{k+1}^2/(\omega_c\eta),$$
$$n_{22}(\lambda_{k+1}, b_{k+1}) = \frac{c^2}{\omega_c^2\eta}\left(\frac{1}{2\lambda_{k+1}^2} + 2b_{k+1}^2\lambda_{k+1}^2\right). \quad (5.6)$$

As with amplitude only modulation, the determinant of the measurement noise covariance matrix is independent of the waveform parameter vector. It can be shown that (5.2) is quadratic in both λ_{k+1}^2 and b_{k+1}, giving a single solution to (5.3) for the LFM pulse. The coefficient of the b_{k+1}^2 term is positive hence the solution is optimal for b_{k+1}; however, the situaton is not as clear for λ_{k+1} and must be resolved using second derivatives. Substituting (5.5) and (5.6) into (5.3) and solving the resultant pair of equations yields

$$b_{k+1}^* = \frac{-\omega_c p_{12}}{2p_{11}},$$
$$\lambda_{k+1}^* = \left(\frac{p_{11}^2}{\omega_c^2(p_{11}p_{22} - p_{12}^2)}\right)^{1/4}.$$

It is straightforward to show

$$\left.\frac{\partial^2 \det(\boldsymbol{S}_{k+1}(\boldsymbol{\theta}_{k+1}))}{\partial\lambda_{k+1}^2}\right|_{\boldsymbol{\theta}_{k+1}=\boldsymbol{\theta}_{k+1}^*} = \frac{4c^2}{p_{11}\eta}(p_{11}p_{22} - p_{12}^2) > 0$$

confirming the above solution is optimal.

The optimal solution for b_{k+1}^* is physically acceptable since b_{k+1} determines the frequency sweep rate for the next transmitted pulse, which may be either positive or negative. Writing

$$\det(\boldsymbol{S}_{k+1}(\boldsymbol{\theta}_{k+1})) = s_{11}s_{22} - s_{12}^2, \quad (5.7)$$

it is clear that the validation gate volume, which is proportional to the square root of $\det(\boldsymbol{S}_{k+1}(\boldsymbol{\theta}_{k+1}))$ [5, p. 168], is minimized by maximizing s_{12}^2, since s_{11} and s_{22} must both be positive. From (5.2), (5.6), and (5.7), $s_{12} = p_{12} - b_{k+1}c^2\lambda_{k+1}^2/(\omega_c\eta)$, hence $|s_{12}|$ is maximized if b_{k+1}^* has the opposite sign to p_{12}.

B. Minimization of Mean Square Tracking Error

The appropriate cost functional for this case is the trace of the tracking error covariance matrix at time $k + 1$ given the measurement sequence up to and including time $k + 1$. Equation (4.2) is a formal specification of this optimization problem. The tracking error covariance matrix is defined by (4.1), however a more convenient form for the current problem is

$$\boldsymbol{P}_{k+1/k+1}(\boldsymbol{\theta}_{k+1}) = \boldsymbol{P}_{k+1/k} - \boldsymbol{P}_{k+1/k}\boldsymbol{H}^T\boldsymbol{S}_{k+1}^{-1}(\boldsymbol{\theta}_{k+1}) \cdot \boldsymbol{H}\boldsymbol{P}_{k+1/k}. \quad (5.8)$$

With $\boldsymbol{H}$ specified by (5.1), the $\boldsymbol{P}_{h/1}$ are 3×3 matrices, while $\boldsymbol{S}_{k+1}(\boldsymbol{\theta}_{k+1})$ is a 2×2 matrix. Expanding (5.8) elementwise, the cost functional becomes

$$\mathrm{Tr}\left(\boldsymbol{P}_{k+1/k+1}(\boldsymbol{\theta}_{k+1})\right) = \mathrm{Tr}(\boldsymbol{P}_{k+1/k}) - \frac{s_{11}(\boldsymbol{\theta}_{k+1})g_{22} + s_{22}(\boldsymbol{\theta}_{k+1})g_{11} - 2s_{12}(\boldsymbol{\theta}_{k+1})g_{12}}{\det(\boldsymbol{S}_{k+1}(\boldsymbol{\theta}_{k+1}))} \quad (5.9)$$

where

$$g_{11} = p_{11}^2 + p_{12}^2 + p_{13}^2,$$
$$g_{12} = p_{11}p_{12} + p_{12}p_{22} + p_{13}p_{23},$$
$$g_{22} = p_{12}^2 + p_{22}^2 + p_{23}^2.$$

Letting

$$f(\boldsymbol{\theta}_{k+1}) = s_{11}(\boldsymbol{\theta}_{k+1})g_{22} + s_{22}(\boldsymbol{\theta}_{k+1})g_{11} - 2s_{12}(\boldsymbol{\theta}_{k+1})g_{12} \quad (5.10)$$

and taking the derivative of (5.9) with respect to the θ_i yields

$$\frac{\partial \operatorname{Tr}\left(\boldsymbol{P}_{k+1/k+1}(\boldsymbol{\theta}_{k+1})\right)}{\partial \theta_i} = \frac{f(\boldsymbol{\theta}_{k+1})\dfrac{\partial \det(\boldsymbol{S}_{k+1}(\boldsymbol{\theta}_{k+1}))}{\partial \theta_i} - \det(\boldsymbol{S}_{k+1}(\boldsymbol{\theta}_{k+1}))\dfrac{\partial f(\boldsymbol{\theta}_{k+1})}{\partial \theta_i}}{(\det(\boldsymbol{S}_{k+1}(\boldsymbol{\theta}_{k+1})))^2}. \tag{5.11}$$

The simultaneous equations defined by setting (5.11) equal to zero can be solved to find the set of solutions corresponding to extreme points of the cost functional. The optimal next transmitted waveform parameter vector $\boldsymbol{\theta}_{k+1}$ is found by substituting the extremum solutions into (5.9) to find the solution with minimum cost.

Closed-form solutions have been obtained for pulses with amplitude only modulation. These waveforms are controlled by the pulse length parameter λ_{k+1}, hence $\boldsymbol{\theta}_{k+1} = \lambda_{k+1}$, and are characterized by measurement noise covariance matrices of the form

$$N(\lambda_{k+1}) = \operatorname{diag}(\alpha\lambda_{k+1}^2, \beta/\lambda_{k+1}^2). \tag{5.12}$$

Here, α and β positive real variables that are inversely dependent on the signal-to-noise ratio of the received pulse. For the one step ahead optimization problems α, β can be considred to be constant at time $k+1$. Each subclass of amplitude only modulated waveforms (e.g., triangular, Gaussian) has different α, β for any given signal-to-noise ratio.

Substituting (5.12) into (5.9) obtains

$$\operatorname{Tr}\left(\boldsymbol{P}_{k+1/k+1}(\lambda_{k+1})\right) = \operatorname{Tr}(\boldsymbol{P}_{k+1/k}) - \frac{\alpha g_{22}\lambda_{k+1}^4 + (p_{11}g_{22} + p_{22}g_{11} - 2p_{12}g_{12})\lambda_{k+1}^2 + \beta g_{11}}{\alpha p_{22}\lambda_{k+1}^4 + (p_{11}p_{22} - p_{12}^2 + \alpha\beta)\lambda_{k+1}^2 + \beta p_{11}}. \tag{5.13}$$

The denominator of (5.13) is positive for all λ_{k+1} since $\boldsymbol{P}_{k+1/k}$ is positive definite $(p_{11}p_{22} - p_{12}^2) > 0$. Putting (5.10) and (5.12) into (5.11), and after much algebraic simplification

$$\frac{\partial \operatorname{Tr}\left(\boldsymbol{P}_{k+1/k+1}(\lambda_{k+1})\right)}{\partial \lambda_{k+1}} = \frac{2\lambda_{k+1}(a\lambda_{k+1}^4 + b\lambda_{k+1}^2 + c)}{\left(\alpha p_{22}\lambda_{k+1}^4 + (p_{11}p_{22} - p_{12}^2 + \alpha\beta)\lambda_{k+1}^2 + \beta p_{11}\right)^2} \tag{5.14}$$

where

$$\begin{aligned} a &= \alpha\left(g_{11}p_{22}^2 - 2g_{12}p_{12}p_{22} + g_{22}(p_{12}^2 - \alpha\beta)\right), \\ b &= 2\alpha\beta(g_{11}p_{22} - g_{22}p_{11}), \\ c &= -\beta\left(g_{11}(p_{12}^2 - \alpha\beta) - 2g_{12}p_{11}p_{12} + g_{22}p_{11}^2\right). \end{aligned}$$

Setting (5.14) to zero and solving for λ_{k+1} yields the extremum points of (5.13). Restricting λ_{k+1} to be real and positive two extrema are immediately apparent, at $\lambda_{k+1} = 0$ and asymptotically as $\lambda_{k+1} \to \infty$. Any other extrema are found by solving

$$a\lambda_{k+1}^4 + b\lambda_{k+1}^2 + c = 0 \tag{5.15}$$

and keeping only the real positive solutions.

In practice, there are both maximum and minimum limits for λ_{k+1} dictated by physical constraints on the tracking system. Denoting these by $\lambda_{\min}$, $\lambda_{\max}$ and the solution to (5.15) by λ_{calc}, a practical algorithm is to solve (5.15) at each time step for λ_{calc} (assuming only one solution), and then to select the optimal transmitted pulse length λ_{k+1}^* according to

$$\lambda_{k+1}^* = \arg \min_{\lambda_{k+1} \in \{\lambda_{\min}, \lambda_{\text{calc}}, \lambda_{\max}\}} \operatorname{Tr}\left(\boldsymbol{P}_{k+1/k+1}(\lambda_{k+1})\right). \tag{5.16}$$

VI. Simulation Results

The update tracker and waveform optimization subsections of the proposed active tracking scheme (Fig. 1) have been simulated for simple tracking scenarios as outlined in the previous section. Consider an underwater stationary transmitting platform operating at a fixed centre transmission frequency of 25 kHz with the speed of sound constant at 1500 m/s. Assume the optimal receiver maintains 100 percent detection of a single true target in the update tracker validation gate; hence, the optimal receiver is simply the measurement noise covariance matrix in (3.11) for the purposes of these simulations. The returned pulse signal-to-noise ratio η in (3.11) is modeled by

$$\eta = (1000/r)^4 \eta_{1000} \tag{6.1}$$

where η_{1000} is the returned pulse signal-to-nose ratio for a target at 1000 m. The range value used in (6.1) is either the observed target range for the update tracker, or the predicted target range for the waveform optimization subsection.

A simple Kalman filter incorporating a maneuver correlation coefficient [22] has been used as the update tracker, where the one-dimensional linear target and measurement models are given by (2.1) and (2.2). The target state vector comprises range, range rate, and radial acceleration, while both range and range rate are observed by the optimal receiver. A 2 s update interval has been chosen (corresponding to 1500 m unambiguous detection range);

hence, the target model system matrices in (2.1) become

$$F = \begin{bmatrix} 1 & 2 & 2 \\ 0 & 1 & 2 \\ 0 & 0 & 0.833 \end{bmatrix}, \qquad G = \begin{bmatrix} 0 \\ 0 \\ 1 \end{bmatrix}.$$

Target process noise variance was set to $Q = 0.01$, while the observation matrix $\boldsymbol{H}$ is defined in (5.1).

Initial simulations were for a single waveform class under a minimum mean square tracking error criterion. The target exhibits a constant radial acceleration of 0.05 g with initial velocity of 5.555 m/s. The returned pulse signal-to-noise ratio at 1000 m was $\eta_{1000} = 0$ dB for simplicity while the minimum and maximum allowable total transmitted pulse lengths were 10 ms and 300 ms, respectively. For the triangular waveforms in these simulations the total pulse length is double the pulse length parameter λ used in previous sections. Minimum pulse length choice is dictated by transmitter/transducer peak power limits while the maximum pulse length specifies minimum detection range for the tracking system, assuming a single transducer array for both reception and transmission. A pulse length of 300 ms corresponds to 225 m minimum detection range for sonar.

Simulation results are shown in Fig. 2 for a target initially at 500 m in range, and in Fig. 3 for a target with an initial range of 1000 m. In both cases the target is accelerating away from the observer. The figures show the selected pulse length at each time k (i.e., the received pulse length at time $k + 1$) and the total mean square tracking error at each time k, defined as $\mathrm{Tr}(\boldsymbol{P}_{k/k})$. The conventional filter responses shown in Fig. 2(b) and Fig. 3(b) are for a standard Kalman filter using the same parameters as the tracker in the waveform adaptive scheme. For the conventional tracker the transmitted waveform was fixed to be a triangular pulse shape with a total pulse length of 11.81 ms, emphasizing range measurement, and was selected to minimize the total mean square measurement noise, i.e., $\lambda_{\mathrm{con}} = \arg\min \mathrm{Tr}(\boldsymbol{N}(\lambda))$ yielding $\lambda_{\mathrm{con}} = 5.905$ ms in this case.

Three phases can be observed in the waveform selection results. Phase one is an initialization phase for the Kalman filter during which $\mathrm{Tr}(\boldsymbol{P}_{k/k})$ is decreasing at successive time steps. If the measurement noise covariance matrix was constant the Kalman filter would be in steady state at the end of this phase. The form of the optimal transmitted waveform pulse length pattern cannot be predicted during this phase as seen for the first three pulse lengths in Fig. 2(a) and the first five pulses in Fig. 3(a). Following initialization is a period where an alternating sequence of long and short pulses is transmitted, confirming the alternating pulse sequence strategy often used in modern radar and sonar systems. A constant stream of long pulses is the final phase for the particular tracking scenario in these simulations. Here, the tracker is demanding the best possible velocity measurements in order to minimize total mean square tracking error.

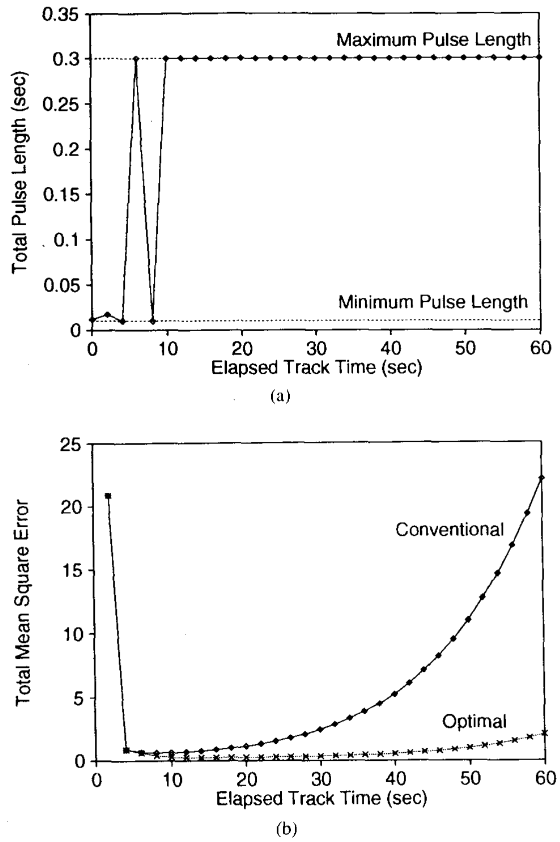

Fig. 2. Tracking error cost functional—triangular CW pulse. Initial range = 500 m, conventional filter pulse length = 11.81 ms; (a) optimal filter transmitted pulse length sequence and (b) $\mathrm{Tr}(\boldsymbol{P}_{k/k})$.

The waveform parameter selection phases are not necessarily distinct, as shown in Fig. 3(a). Here, two long pulses are transmitted, followed by a short pulse, before the final phase commences demonstrating the boundary region in the optimization scenario between alternating and long pulse only transmission sequences. Figs. 2 and 3 show the dependence of the selected waveform pattern on initial signal-to-noise ratio (initial range in this case), although the patterns have the similar phases due to the similarity of the tracking scenario in the two cases. A quite different transmitted waveform pattern would be obtained if, for example, an approaching, then receding target was tracked. Also apparent in the simulation results is the degradation in total mean square tracking error for the conventional tracking filter as the signal-to-noise ratio deteriorates (target is accelerating away from the observer), whereas the optimal waveform selection scheme appears to be less sensitive to signal-to-noise ratio.

The same target track scenario was also used to demonstrate the multiple waveform class capability of the proposed optimal waveform selection scheme. Utilizing minimum validation gate volume as the chosen cost criterion allowed the use of closed-form solutions for amplitude only modulation and amplitude with linear frequency

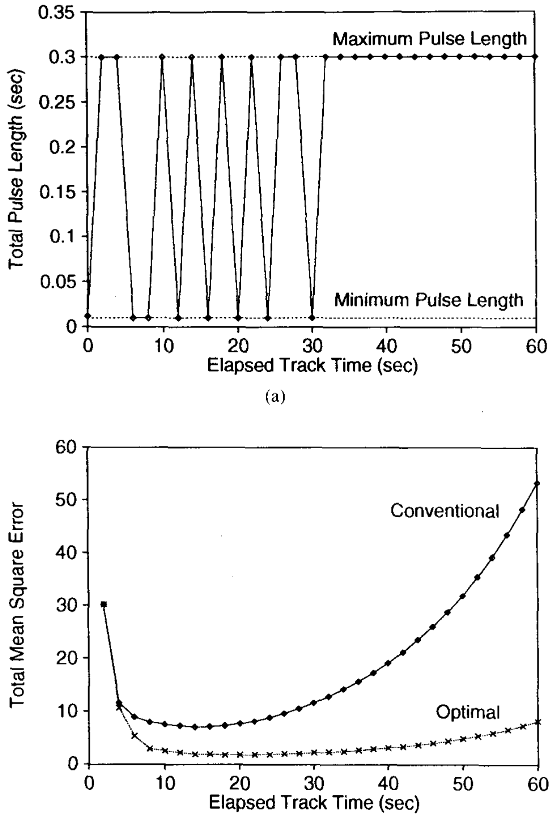

Fig. 3. Tracking error cost functional—triangular CW pulse. Initial range = 1000 m, conventional filter pulse length = 11.81 ms; (a) optimal filter transmitted pulse length sequence and (b) $\mathrm{Tr}(\boldsymbol{P}_{k/k})$.

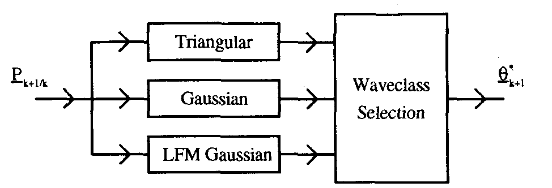

Fig. 4. Waveform optimization subsection block structure for multiple waveform classes.

modulation waveforms previously obtained. The waveform optimization block in Fig. 1 can be easily expanded to allow multiple waveform classes, as illustrated in Fig. 4. Individual class waveform selection is performed in parallel with the final waveform selected according to which of the individual class selections yields the lowest cost for the next transmitted waveform. The waveform parameter vector $\boldsymbol{\theta}_{k+1}$ now contains a waveform class identifier in addition to pulse length and LFM sweep rate.

The waveclass switching ability of the optimal waveform selection algorithm is clearly illustrated in Fig. 5(a), for an initial target range of 500 m. In this figure, class 1 is triangular amplitude only modulation, class 2 is Gaussian amplitude-only modulation, and class 3 is Gaussian amplitude and linear frequency modulation. The pulse lengths shown in Fig. 5(b) are total or effective pulse lengths for the individual waveforms. Effective pulse length in the case of the Gaussian waveforms is determined by the point where the waveform amplitude has dropped to 0.1 percent of the peak waveform amplitude. In terms of the Gaussian waveform parameter, the effective pulse length is 7.4338λ, where λ is the Gaussian waveform pulse length parameter (see Appendix B). Fig. 5(c) contains the LFM sweep rate for each transmitted pulse, while Fig. 5(d) shows a comparison of the validation gate volume for the optimal waveform selection tracker against a conventional single waveform tracker. In this case, the conventional waveform used was a Gaussian amplitude only modulated pulse with an effective pulse length of 12 ms.

VII. Discussion

In this paper we have concentrated on simple one-dimensional single-target tracking scenarios where the measurement noise covariance matrix is specified completely by the narrowband time-frequency ambiguity function. The demonstrated optimal waveform selection algorithms have only considered local (one step ahead) optimization problems under the constraint of a time-invariant Kalman filter tracker. However the underlying concept in this work is applicable to a wide range of active transmission target tracking scenarios. Potential extensions of the basic ideas are briefly discussed below.

1) We have derived our waveform selection algorithms based on specific measures of target tracking performance, either minimizing the mean square tracking error or the size of the target validation gate in measurement space. The general ideas are also valid for other cost functionals, depending on the user requirements for the particular tracking system. One example is to select the next transmitted waveform so as to increase track detection decision speed, which is of great importance in surveillance situations.
2) The waveform selection concept, a presented in this paper, is not limited to a single tracking algorithm as it simply modifies assumptions about the measurement noise convariance matrix used by the tracking algorithm. Modification of the probabilistic data association filter (PDAF) to include waveform selection is currently under investigation [14].
3) The extension from a single sensor system to a multiple sensor system (for certain situations) is straightforward. Let y_i, T_i, and N_i be the measurement vector, parameter transformation matrix, and measurement noise covariance matrix at the ith sensor, respectively. Assuming measurement independence between the individual sensors then the system measurement vector is $y^T = [y_1^T, y_2^T, \cdots, y_m^T]$, while the system parameter transformation matrix and measurement noise covariance matrix are the

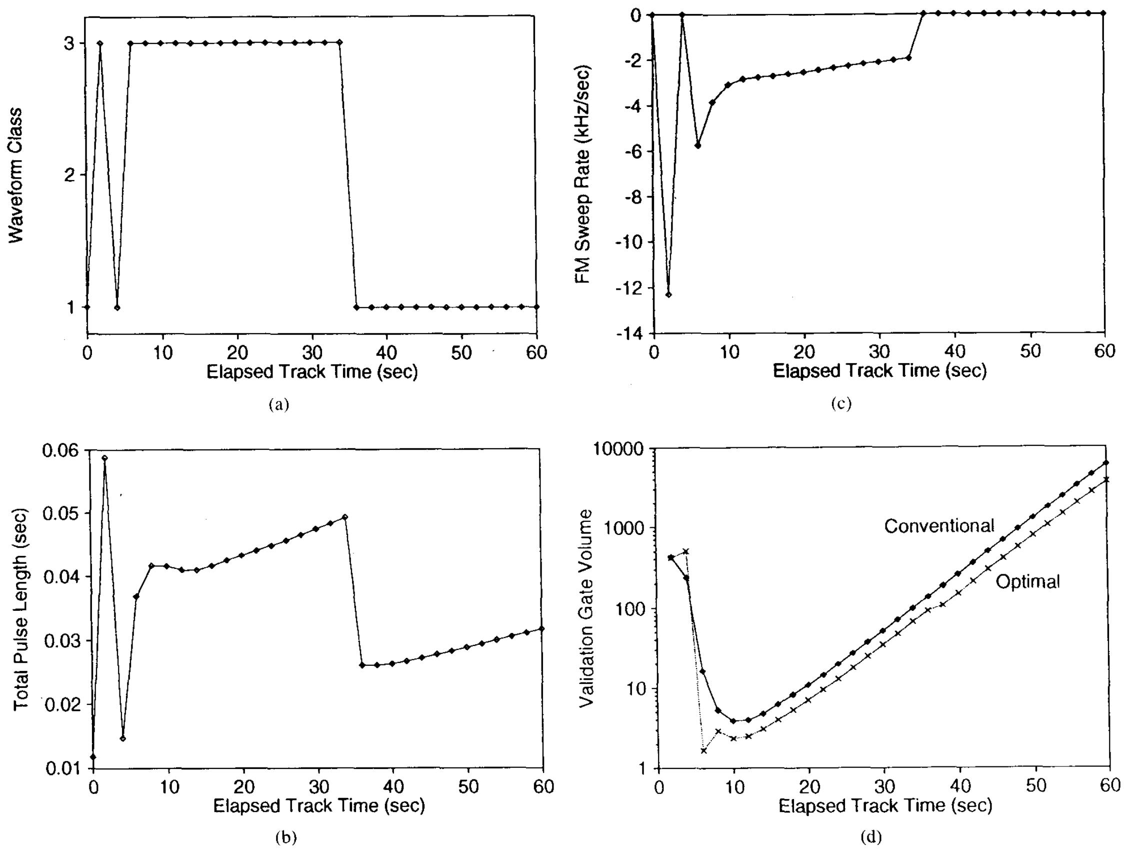

Fig. 5. Multiple waveform class simulation example—validation gate volume cost functional. Initial range = 500 m, conventional filter pulse length = 12 ms; (a) transmitted waveform class, (b) transmitted pulse length sequence, (c) transmitted pulse LFM sweep rate, and (d) $\det(S_k)$.

block diagonal matrices $T = \mathrm{diag}(T_1, T_2, \cdots, T_m)$ and $N = \mathrm{diag}(N_1, N_2, \cdots, N_m)$, where m is the number of sensors. Similar extensions may be made to the tracking filter equations of the Section IV to yield system wide, rather than individual sensor, tracking equations. The selected waveform is then optimal for the overall system, assuming a single transmitted waveform is used at each time step.

4) The measurement noise covariance matrix was derived in Section III for range and range rate measurements only, allowing the covariance matrix to be characterized by the time-frequency ambiguity function. In a practical system, azimuth and elevation angles are also measured, leading to a generalized ambiguity function [26, p. 337]. For this case the measurement noise covariance matrix is still defined by Lemma 3.1. For example, consider the measurement vector $y = [r\ \dot{r}\ \phi]^T$, where the angle estimate has variance σ_ϕ^2 and is independent of the range and range rate estimates. If T_A and N_A are the 2×2 parameter transformation and measurement noise covariance matrices in (3.11), then the extended versions of these matrices are $T = \mathrm{diag}(T_A, 1)$ and $N = \mathrm{diag}(N_A, \sigma_\phi^2)$. Naturally, the uncertainty principle results hold only for the time-frequency submatrix N_A of the extended measurement noise covariance matrix obtained from the generalized ambiguity function.

5) The narrow-band approximation of replacing the true Doppler effect of a time compression or expansion by a Doppler shift is often invalid for sonar systems due to the wide bandwidths, compared to transmission frequencies, used in such systems. To implement the true Doppler effect the narrow-band received envelope (3.1) must be replaced by the expression

$$\tilde{r}(t) = \sqrt{E_R}\, e^{j\phi} \tilde{s}(\beta_0 t - \tau_0) e^{j\omega_c(\beta_0 t - \tau_0)} + \tilde{n}(t)$$

where $\beta_0 = (c - \dot{r}_0)/(c + \dot{r}_0)$ and $\tau_0 = 2r_0/(c + \dot{r}_0)$. These expressions assume a constant target range rate, that is $r(t) = r_0 + \dot{r}_0 t$, where $r(t)$ is the target range. As with the narrow-band approximation a matched filter can be formed for the received pulse, thus if β and τ are the Doppler parameters for the matched filter we can form an wide-band ambiguity function using a similar argument to that in obtaining the narrow-band ambiguity function (3.2) to yield [11, 24]

$$A_w(\tau', \gamma) = \int_{-\infty}^{\infty} \tilde{s}(t)\tilde{s}^*(\gamma t + \tau')e^{j\omega_c((1-\gamma)t-\tau')}\,dt.$$

For this expression $\gamma = \beta/\beta_0$, $\tau' = \gamma\tau_0 - \tau$, and $A_w(\tau', \gamma)$ is a maximum at $A_w(0, 1)$. The incorporation of the wide-band ambiguity function into the optimal waveform selection algorithm is currently under investigation.

6) The algorithm presented in this paper is for active transmission systems with constant pulse repetition frequency and constant pulse energy. These two assumptions have allowed us to solve the local or one step ahead waveform selection problem. A more advanced algorithm would also provide solutions to the optimal waveform selection when the above constraints are relaxed. To achieve this simultaneous peak power and average power constraints need to be imposed in a similar fashion to the constraints imposed in [1], and [21] when obtaining solutions for the optimal waveform design problem. Unlike the control theoretic approach used in [1] and [21], and most other waveform design methods [8], we are not limited to amplitude only modulated waveforms modeled using a multiplicative waveform control variable. This problem may be considered as the global optimal waveform selection problem.

7) Within the constraint of a linear (Kalman) tracking filter tracking error covariance matrix can be predicted at any future time step, opening a wide range of potential m-step ahead optimization problems for waveform selection. For example, the two step ahead smoothed tracking error covariance matrix is dependent on both $\boldsymbol{\theta}_{k+1}$ and $\boldsymbol{\theta}_{k+2}$ via

$$\begin{aligned}P_{k+2/k+2}(\boldsymbol{\theta}_{k+2}, \boldsymbol{\theta}_{k+1}) &= P_{k+2/k+1}(\boldsymbol{\theta}_{k+1}) - P_{k+2/k+1}(\boldsymbol{\theta}_{k+1})H^T \\ &\quad \cdot S_{k+2}^{-1}(\boldsymbol{\theta}_{k+2}, \boldsymbol{\theta}_{k+1})HP_{k+2/k+1}(\boldsymbol{\theta}_{k+1}),\end{aligned}$$

where

$$P_{k+2/k+1}(\boldsymbol{\theta}_{k+1}) = FP_{k+1/k+1}(\boldsymbol{\theta}_{k+1})F^T + GQ_{k+1}G^T$$

and

$$S_{k+2}(\boldsymbol{\theta}_{k+2}, \boldsymbol{\theta}_{k+1}) = HP_{k+2/k+1}(\boldsymbol{\theta}_{k+1})H^T + N(\boldsymbol{\theta}_{k+2}).$$

$N(\boldsymbol{\theta}_{k+1})$ is implicitly included in the above expression for $P_{k+2/k+2}(\boldsymbol{\theta}_{k+2}, \boldsymbol{\theta}_{k+1})$ via $P_{k+1/k+1}(\boldsymbol{\theta}_{k+1})$, as shown in (4.1). Having previously derived expressions for one step ahead scalar cost functions in terms of the waveform parameter vector (4.2), (4.3), we are able to pose the following two optimization problems for m-step ahead optimal waveform selection. The m-step ahead problems are

1):

$$\boldsymbol{\theta}_{k+1}^*, \cdots, \boldsymbol{\theta}_{k+m}^* = \arg \min_{\boldsymbol{\theta}_{k+1}, \cdots, \boldsymbol{\theta}_{k+m}} \sum_{i=k+1}^{k+m} \operatorname{Tr}\left(P_{i/i}(\boldsymbol{\theta}_i)\right)$$

2):

$$\boldsymbol{\theta}_{k+1}^*, \cdots, \boldsymbol{\theta}_{k+m}^* = \arg \min_{\boldsymbol{\theta}_{k+1}, \cdots, \boldsymbol{\theta}_{k+m}} \sum_{i=k+1}^{k+m} \det\left(S_i(\boldsymbol{\theta}_i)\right)$$

where $\{\boldsymbol{\theta}_{k+1}^*, \cdots, \boldsymbol{\theta}_{k+m}^* \in \boldsymbol{\Theta}\}$ are the transmitted waveform parameter vectors for the next m transmitted pulses. In most situations of practical interest this requires brute force optimization techniques, however in some simple situations it appears that closed form solutions may be possible.

8) For tracking scenarios where analytic solutions to the local optimization problem are intractable, and a numerical optimization is undesirable, it is straightforward to apply a standard gradient descent algorithm to only partially solve the optimization problem at each step. While not providing the optimal waveform selection at each time step these algorithms will provide an improvement in the cost at each step with considerably reduced computational effort. The potential of such algorithms is due to the ease with which the derivatives of the cost functionals with respect to the optimization variables can be calculated. For example, consider the total mean square tracking error cost functional (4.2). Here, the first derivative of the cost functional with respect to any element of the waveform parameter vector is easily calculated using (see Appendix E for details)

$$\begin{aligned}\frac{\partial \operatorname{Tr}\left(P_{k+1/k+1}(\boldsymbol{\theta}_{k+1})\right)}{\partial \theta_i} &= \operatorname{Tr}\left(P_{k+1/k}H^T S^{-1}(\boldsymbol{\theta}_{k+1})\frac{\partial N(\boldsymbol{\theta}_{k+1})}{\partial \theta_i}\right. \\ &\quad \left.\cdot S^{-1}(\boldsymbol{\theta}_{k+1})HP_{k+1/k}\right). \end{aligned} \tag{7.1}$$

The second derivatives can be evaluated similarly to yield

$$\begin{aligned}\frac{\partial^2 \operatorname{Tr}(P_{k+1/k+1})}{\partial \theta_i^2} &= \operatorname{Tr}\left(P_{k+1/k}H^T S^{-1}\left\{\frac{\partial^2 N}{\partial \theta_i^2} - 2\frac{\partial N}{\partial \theta_i}S^{-1}\frac{\partial N}{\partial \theta_i}\right\}\right. \\ &\quad \left.\cdot S^{-1}HP_{k+1/k}\right),\end{aligned} \tag{7.2}$$

$$\begin{aligned}\frac{\partial^2 \operatorname{Tr}(P_{k+1/k+1})}{\partial \theta_i\, \partial \theta_j} &= \operatorname{Tr}\left(P_{k+1/k}H^T S^{-1}\left\{\frac{\partial^2 N}{\partial \theta_i\, \partial \theta_j} - \frac{\partial N}{\partial \theta_i}S^{-1}\frac{\partial N}{\partial \theta_j}\right.\right. \\ &\quad \left.\left. - \frac{\partial N}{\partial \theta_j}S^{-1}\frac{\partial N}{\partial \theta_i}\right\}S^{-1}HP_{k+1/k}\right).\end{aligned} \tag{7.3}$$

For clarity, the explicit dependence of N, $P_{k+1/k+1}$ and S on θ_{k+1} is not shown in (7.2) and (7.3). When included in an appropriate gradient descent algorithm, the general formulas (7.1), (7.2), and (7.3), may replace the specialized formulas of the unique sensor case reported in Section V.

VIII. Conclusion

Optimal adaptive waveform selection for active transmission tracking systems has been reexamined from a systems engineering viewpoint. Assuming an optimal detector for the first stage of the system receiver allows the measurement noise covariance matrix at the output of the detector to have an explicit dependence on the transmitted waveform parameters. This dependence is exploited to form tracking system performance measures that are directly dependent on the nex transmitted waveform, thus allowing the formulation of optimization problems to select the best waveform for transmission. Simulation of a simple tracking scenario demonstrated the potential improvement in tracking performance available through optimal waveform selection. We have also developed closed-form solutions (under some restricted circumstances), hence avoiding the need for numerical optimization routines in the final adaptive algorithms. The general technique appears to be readily applicable to a wide range of current target tracking situations. A number of possible extensions to the present work have also been outlined.

Appendix A
Derivation of Equation (3.9)

Assuming $\bar{\omega}, \bar{t} = 0$, (3.6) becomes

$$\overline{\omega t} = -\left.\frac{\partial^2 A(\tau,\nu)}{\partial\tau\,\partial\nu}\right|_{\tau,\nu=0}. \tag{A.1}$$

The ambiguity function can be written as

$$A(\tau,\nu) = e^{-j\tau\nu/2}B(\tau,\nu)$$

where

$$B(\tau,\nu) = \int_{-\infty}^{\infty} \tilde{s}(t)\tilde{s}^*(t+\tau)e^{-j\nu t}\,dt. \tag{A.2}$$

It is straightforward to show

$$\left.\frac{\partial^2 A(\tau,\nu)}{\partial\tau\,\partial\nu}\right|_{\tau,\nu=0} = -\frac{j}{2} + \left.\frac{\partial^2 B(\tau,\nu)}{\partial\tau\,\partial\nu}\right|_{\tau,\nu=0},$$

where differentiating (A.2) with respect to both τ and ν, and evaluating at $\tau = \nu = 0$, obtains

$$\left.\frac{\partial^2 A(\tau,\nu)}{\partial\tau\,\partial\nu}\right|_{\tau,\nu=0} = -j/2 - j\int_{-\infty}^{\infty} t\tilde{s}(t)\tilde{s}'^*(t)\,dt. \tag{A.3}$$

Here $x'(t)$ is taken to mean $dx(t)/dt$. This expression can be further simplified by writing $\tilde{s}(t)$ in magnitude and phase form as $\tilde{s}(t) = a(t)\exp(j\varphi(t))$, where $a(t) = |\tilde{s}(t)|$. Using this representation the derivative of $\tilde{s}(t)$ with respect to t becomes

$$\tilde{s}'^*(t) = a'(t)e^{-j\varphi(t)} - j\varphi'(t)a(t)e^{-j\varphi(t)},$$

and hence

$$\int_{-\infty}^{\infty} t\tilde{s}(t)\tilde{s}'^*(t)\,dt = \int_{-\infty}^{\infty} ta(t)a'(t)\,dt - j\int_{-\infty}^{\infty} t\varphi'(t)a^2(t)\,dt. \tag{A.4}$$

But, integrating by parts, the first integral on the right-hand side of this expression is

$$\int_{-\infty}^{\infty} ta(t)a'(t)\,dt = \frac{1}{2}[ta^2(t)]_{-\infty}^{\infty} - \frac{1}{2}\int_{-\infty}^{\infty} a^2(t)\,dt = -\frac{1}{2} \tag{A.5}$$

since

$$\int_{-\infty}^{\infty} a^2(t)\,dt = \int_{-\infty}^{\infty} |\tilde{s}(t)|^2\,dt = 1.$$

Substituting (A.3), (A.4), and (A.5) into (A.1) obtains the final result

$$\overline{\omega t} = \int_{-\infty}^{\infty} t\varphi'(t)|\tilde{s}(t)|^2\,dt$$

where

$$\tilde{s}(t) = |\tilde{s}(t)|e^{j\varphi(t)}.$$

Appendix B
Measurment Noise Covariance Matrix Calculation for Selected Waveform Classes

Parameters for example waveform classes, where the measurement vector is $y = [r\ \dot{r}]^T$ and $T = \operatorname{diag}(c/2, c/2\omega_c)$. For all three waveform classes below the time and frequency origins have been chosen so that $\bar{t} = 0$ and $\bar{\omega} = 0$. As expected, $\overline{\omega t} = 0$ for the two purely amplitude-modulated waveforms since this measures the amount of frequency modulation in the signal pulse [13, p. 19].

1) Triangular Pulse—CW:

$$\tilde{s}(t) = \begin{cases} \sqrt{\dfrac{3}{2\lambda}}\left(1 - \dfrac{|t|}{\lambda}\right) & -\lambda < t < \lambda \\ 0 & \text{otherwise} \end{cases}$$

$$\tilde{S}(\omega) = \sqrt{\frac{3\lambda}{2}}\,\operatorname{sinc}^2\left(\frac{\omega\lambda}{2}\right)$$

$$\overline{\omega^2} = 3/\lambda^2, \quad \overline{t^2} = \lambda^2/10, \quad \overline{\omega t} = 0$$

$$\det(U(\lambda)) = 3/10$$

$$N(\lambda) = \begin{bmatrix} \dfrac{c^2\lambda^2}{12\eta} & 0 \\ 0 & \dfrac{5c^2}{2\omega_c^2\lambda^2\eta} \end{bmatrix}$$

$$\det(N(\lambda)) = \frac{5c^4}{24\omega_c^2\eta^2}.$$

2) Gaussian Pulse—CW:

$$\tilde{s}(t) = \left(\frac{1}{\pi\lambda^2}\right)^{1/4}\exp\left(\frac{-t^2}{2\lambda^2}\right)$$

$$\tilde{S}(\omega) = (4\pi\lambda^2)^{1/4}\exp\left(\frac{-\omega^2\lambda^2}{2}\right)$$

$$\overline{\omega^2} = 1/2\lambda^2, \quad \overline{t^2} = \lambda^2/2, \quad \overline{\omega t} = 0$$

$$\det(U(\lambda)) = 1/4$$

$$N(\lambda) = \begin{bmatrix} \dfrac{c^2\lambda^2}{2\eta} & 0 \\ 0 & \dfrac{c^2}{2\omega_c^2\lambda^2\eta} \end{bmatrix}$$

$$\det(N(\lambda)) = \frac{c^4}{4\omega_c^2\eta^2}.$$

3) Gaussian Pulse—LEM:

$$\tilde{s}(t) = \left(\frac{1}{\pi\lambda^2}\right)^{1/4} \exp\left(-\left(\frac{1}{2\lambda^2} - jb\right)t^2\right)$$

$$\tilde{S}(\omega) = \frac{(4\pi\lambda^2)^{1/4}}{\sqrt{1-2jb\lambda^2}} \exp\left(\frac{-\omega^2\lambda^2}{2(1-2jb\lambda^2)}\right)$$

$$\overline{\omega^2} = (1/2\lambda^2) + 2b^2\lambda^2, \quad \overline{t^2} = \lambda^2/2, \quad \overline{\omega t} = b\lambda^2$$

$$\det(U(\theta)) = 1/4$$

$$N(\theta) = \begin{bmatrix} \dfrac{c^2\lambda^2}{2\eta} & \dfrac{-c^2 b\lambda^2}{\omega_c \eta} \\ \dfrac{-c^2 b\lambda^2}{\omega_c\eta} & \dfrac{c^2}{\omega_c^2\eta}\left(\dfrac{1}{2\lambda^2} + 2b^2\lambda^2\right) \end{bmatrix}$$

$$\det(N(\theta)) = \frac{c^4}{4\omega_c^2\eta^2}$$

where

$$\theta = [\lambda \ b]^T.$$

Appendix C

Proof of Lemma 3.3: Let $N(\theta_1)$ and $N(\theta_2)$ be noise covariance matrices for waveforms in class C, i.e., $\theta_1, \theta_2 \in \Theta_C$. There exists, [18, p. 21], a nonsingular matrix C and a positive definite diagonal matrix $\Lambda = \operatorname{diag}(\lambda_1, \cdots, \lambda_n)$ such that

$$N(\theta_1) = CC^T, \qquad N(\theta_2) = C\Lambda C^T,$$

and

$$N(\theta_2) - N(\theta_1) = C(\Lambda - I)C^T.$$

By Sylvester's Law of Inertia, [23], $N(\theta_2) - N(\theta_1)$ will have the same number of positive, negative and zero eigenvalues as $\Lambda - I$. Since $\det N(\theta_1) = \det N(\theta_2)$, then $\det \Lambda = \prod \lambda_i = \det I = 1$ and at least one $\lambda_i < 1$. Thus, $N(\theta_2) - N(\theta_1)$ has at least one negative eigenvalue and cannot be positive definite. Hence, $N(\theta_1) < N(\theta_2)$ cannot hold for any $\theta_1, \theta_2 \in \Theta_C$. □

Appendix D

Proof of Lemma 4.1: If $N(\theta_1)$, $N(\theta_2)$ are the measurement noise covariance matrices corresponding to the waveform parameter vectors θ_1, θ_2 and P is the predicted tracking error covariance matrix then we can use (4.1) to write (P symmetric)

$$P(\theta_2) - P(\theta_1) = PH^T\left[(HPH^T + N(\theta_1))^{-1} - (HPH^T + N(\theta_2))^{-1}\right]HP.$$

From Lemma 3.3, $N(\theta_2) - N(\theta_1)$ cannot be positive definite, hence $(HPH^T + N(\theta_2)) - (HPH^T + N(\theta_1))$ cannot be positive definite. This implies [18, p. 21] $(HPH^T + N(\theta_1))^{-1} - (HPH^T + N(\theta_2))^{-1}$ also cannot be positive definite, hence, by Sylvester's Law of Inertia [23, p. 257], $P(\theta_2) - P(\theta_1)$ cannot be positive definite. Thus, there does not exist a $\theta_1 \in \Theta_C$ such that $P(\theta_1) < P(\theta_2)$ for all $\theta_2 \in \Theta_C$. □

Appendix E
Derivation of Equations (7.1), (7.2), and (7.3)

The total mean square tracking error cost functional is given by $\operatorname{Tr}(P_{k+1/k+1}(\theta_{k+1}))$, where from (5.8)

$$P_{k+1/k+1}(\theta_{k+1}) = P_{k+1/k} - P_{k+1/k}H^T \cdot S_{k+1}^{-1}(\theta_{k+1})HP_{k+1/k}. \quad \text{(E.1)}$$

The derivative of the cost functional with respect to the elements of the waveform parameter vector θ_{k+1} is given by

$$\frac{\partial(\operatorname{Tr}(P_{k+1/k+1}(\theta_{k+1})))}{\partial\theta_i} = \operatorname{Tr}\left(\frac{\partial P_{k+1/k+1}(\theta_{k+1})}{\partial\theta_i}\right), \quad \text{(E.2)}$$

since the trace and derivative operators are linear and commute [18, p. 148]. Calculating the derivative in the RHS of (E.2) yields

$$\frac{\partial P_{k+1/k+1}(\theta_{k+1})}{\partial\theta_i} = -P_{k+1/k}H^T\frac{\partial S^{-1}(\theta_{k+1})}{\partial\theta_i}HP_{k+1/k}. \quad \text{(E.3)}$$

Also, for any real symmetric matrix $X(\theta)$ [18, p. 183]

$$\frac{\partial(X^{-1}(\theta))}{\partial\theta_i} = -X^{-1}(\theta)\frac{\partial X(\theta)}{\partial\theta_i}X^{-1}(\theta). \quad \text{(E.4)}$$

Using (E.3), (E.4), and noting that $S(\theta_{k+1}) = HP_{k+1/k}H^T + N(\theta_{k+1})$, obtains the final result shown in (7.1).

References

[1] M. Athans and F. C. Schweppe, "Optimal waveform design via control theoretic principles," *Inform. Control*, vol. 10, pp. 335–377, Apr. 1967.
[2] M. Athans and E. Tse, "A direct derivation of the optimal linear filter using the maximum principle," *IEEE Trans. Automat. Contr.*, vol. AC-12, pp. 690–698, Dec. 1967.
[3] R. F. Barrett and D. A. Holdsworth, "Frequency tracking using hidden Markov models with amplitude and phase information," *IEEE Trans. Signal Process.*, vol. 41, pp. 2965–2976, Oct. 1993.
[4] Y. Bar-Shalom, L. J. Campo, and P. B. Luh, "From receiver operating characteristic to system operating characteristic: Evaluation of a track formation system," *IEEE Trans. Automat. Contr.*, vol. AC-35, pp. 172–179, Feb. 1990.
[5] Y. Bar-Shalom and T. E. Fortmann, *Tracking and Data Association.* New York: Academic, 1988.
[6] R. E. Bethel and R. G. Rahikka, "An optimal first-order time delay tracker," *IEEE Trans. Aerosp. Electron. Syst.*, vol. AES-23, pp. 718–725, Nov. 1987.
[7] ——, "Optimal time delay detection and tracking," *IEEE Trans. Aerosp. Electron. Syst.*, vol. AES-26, pp. 700–711, Sept. 1990.
[8] F. Daum, "A system approach to multiple target tracking," in *Multitarget-Multisensor Tracking: Applications and Advances*, Y. Bar-Shalom, Ed. Boston: Artech House, vol. 2, 1992, pp. 149–181.
[9] R. J. Evans, A. Cantoni, and B. D. O. Anderson, "Theoretical aspects of optimal autocorrelation synthesis," *Inform. Sci.*, vol. 22, pp. 171–199, 1980.
[10] T. E. Fortmann *et al.*, "Detection thresholds for tracking in clutter —A connection between estimation and signal processing," *IEEE Trans. Automat. Contr.*, vol. AC-30, pp. 221–228, Mar. 1985.
[11] R. L. Gassner and G. R. Cooper, "Note on a generalized ambiguity function," *IEEE Trans. Inform. Theory*, vol. IT-13, no. 1, p. 126, Jan. 1967.
[12] T. H. Glisson, C. I. Black, and A. P. Sage, "On sonar signal analysis," *IEEE Trans. Aerosp. Electron. Syst.*, vol. AES-6, pp. 37–49, Jan. 1970.
[13] C. W. Helstrom, *Statistical Theory of Signal Detection*, 2nd ed. New York: Pergamon, 1966.
[14] D. J. Kershaw and R. J. Evans, "Adaptive waveform selection for tracking in clutter," in *Proc. 1994 Amer. Cont. Conf.*, Baltimore, Maryland, 1994.

[15] D. Lerro and Y. Bar-Shalom, "Automated tracking with target amplitude information" in *Proc. 1990 Amer. Cont. Conf.*, San Diego, CA, 1990.

[16] R. J. McAulay and J. R. Johnson, "Optimal mismatched filter design for radar ranging, detection, and resolution," *IEEE Trans. Inform. Theory*, vol. IT-17, pp. 696–701, Nov. 1971.

[17] P. J. McLane, P. H. Wittke, and C. K.-S. Ip, "Least mean-square-error adaptation of parameters in track-while-scan radar systems," in *Proc. IEEE Int. Radar Conf.*, Washington, 1980, pp. 451–457.

[18] J. R. Magnus and H. Neudecker, *Matrix Differential Calculus with Applications in Statistics and Econometrics*. New York: Wiley, 1988.

[19] R. L. Mitchell and A. W. Rihaczek, "Matched filter responses of the linear FM waveform," *IEEE Trans. Aerosp. Electron. Syst.*, vol. AES-4, pp. 417–432, May 1968.

[20] V. Nagarajan, M. R. Chidambara, and R. N. Sharma, "New approach to improved detection and tracking performance in track-while-scan radars, part 1: Introduction and review," *IEE Proc., Pt. F*, vol. 134, no. 1, pp. 89–92, Feb. 1987.

[21] F. C. Schweppe and D. L. Gray, "Radar signal desig subject to simultaneous peak and average power constraints," *IEEE Trans. Inform. Theory*, vol. IT-12, pp. 13–26, Jan. 1966.

[22] R. A. Singer, "Estimating optimal tracking filter performance for manned manoeuvring targets," *IEEE Trans. Aerosp. Electron. Syst.*, vol. AES-6, pp. 472–783, July 1970.

[23] G. Strang, *Linear Algebra and Its Applications*, 2nd ed. New York: Academic, 1980.

[24] D. A. Swick, "Wideband ambiguity function of pseudo-random sequences: An open problem," *IEEE Trans. Inform. Theory*, vol. IT-14, pp. 602–603, July 1968.

[25] H. L. Van Trees, "Optimum signal design and processing for reverberation limited environments," *IEEE Trans. Mil. Elect.*, pp. 212–229, July 1965.

[26] H. L. Van Trees, *Detection, Estimation and Modulation Theory, Part III*. New York: Wiley, 1971.

[27] C. H. Wilcox, "The synthesis problem for radar ambiguity functions," *MRC Tech. Summary Rep. 157*, Univ. Wisconsin, Madison, Apr. 1960; reprinted in R. E. Blahut, W. Miller, Jr., and C. H. Wilcox, *Radar and Sonar, Part I*, IMA Volumes in Mathematics and Applications, vol. 32. New York: Springer-Verlag, 1991, pp. 229–260.